

Plane wave propagation in finite 2-2 composites

Wenwu Cao^{a)} and Wenkang Qi

Materials Research Laboratory, The Pennsylvania State University, University Park, Pennsylvania 16802

(Received 4 November 1994; accepted for publication 19 June 1995)

A common practice in the study of wave propagation in stratified structures is to use the Floquet (or Bloch) condition to derive the dispersion relation, leading to the passband and stopband structures. However, the Floquet condition is valid only for an infinite system while a real system always has finite dimensions. We report a study on wave propagation in a finite 2-2 composite by using the transfer (T) matrix technique. Through introducing a new definition for the dispersion relation using the T matrix, the passbands and stopbands are calculated for a finite system without the Floquet condition. The formation of stopbands and passbands with the increase of composite size can now be clearly seen. The spatial profile of the vibration pattern inside a finite composite can also be calculated using this technique, which reveals strong edge effects. The effects of randomization on the wave localization in a 2-2 composite are also studied. © 1995 American Institute of Physics.

I. INTRODUCTION

The dynamic behavior of piezoelectric composites has attracted the attention of many researchers after it has been successfully applied to under water acoustics and medical ultrasound imaging.¹⁻¹⁹ Conceptual understanding was achieved in many aspects for composite structures, and some guidelines for composite transducer design were also developed. However, there are still many unanswered questions regarding the composite structure. Some of the most fundamental and interesting topics include wave propagation inside the composite structure, mode coupling, and band structures for a finite system.

Several methods were introduced in the study of wave propagation in periodic composites, such as the T -matrix method,^{10,14,16,20} the effective medium method,^{13,14} and the finite element method.¹⁵⁻¹⁷ Each method has certain merits but also limitations. Among these methods, the finite element method is the most powerful method which can deal with complex geometry. However, it is limited by the power of the computer, and the results from the finite element analysis often do not lead to a clear conceptual understanding of the physical origin of the observed phenomena. Another accurate method is the transfer matrix (T -matrix) method, which is especially suitable to study wave propagation in one-dimensional layered structures, such as 2-2 composites. The T -matrix method has been used to study the dilational Lamb wave in a 2-2 composite in conjunction with the Floquet theory.^{10,14,16,20} Many interesting results, including the band structures, were obtained, which have provided conceptual understanding of some wave propagation characteristics in composites.

Wave propagation in stratified structures, such as a 2-2 composite illustrated in Fig. 1, have been studied extensively using transfer matrix.²¹⁻²⁵ In the past, band structures were calculated by using a combination of T matrix and the Floquet theory, because the traditional T -matrix method alone does not provide enough information to determine the band structures. The problem of Floquet theory is that it is valid only for an infinite system. Therefore, the band structures

obtained in all the previous studies do not accurately describe the wave propagation characteristics in finite systems. It is predictable that the Floquet condition will be strongly violated when a composite contains only a few cells. Focusing on this problem, we introduce an extension to the T -matrix technique which enables the T -matrix technique to calculate the band structures for a finite stratified structures, such as 2-2 composites, without using Floquet condition.

As an example, we will consider the transverse wave propagation in a 2-2 composite; one can easily calculate the longitudinal wave analogously.

II. T MATRIX AND THE NEW DISPERSION RELATION

As mentioned above, the main objective of this study is to derive a substitute for the Floquet condition to calculate the band structures for a finite stratified structure. We begin with a brief review on the T -matrix technique and then introduce some new definitions.

Assuming a shear acoustic plane wave $\psi(x,t)$ enters a ceramic-polymer composite system shown in Fig. 1 from the left at $x=0$, we can write the wave function at the n th cell in the following form:

$$\psi_n = A_n e^{i(\omega t - k_p x)} + B_n e^{i(\omega t + k_p x)},$$
$$(n-1)d < x < nd - a \quad (\text{in polymer}); \quad (1)$$

$$\psi_n = C_n e^{i(\omega t - k_c x)} + D_n e^{i(\omega t + k_c x)},$$
$$nd - a < x < nd \quad (\text{in ceramic}); \quad (2)$$

where

$$k_m = \omega \sqrt{\rho_m / c_{55}^m} \quad (m = p, c) \quad (3)$$

is the wave number, a and b are the thickness of the ceramic layer and polymer layer, respectively, $a + b = d$ is the period of the cell (see Fig. 1), ω is the angular frequency, ρ_m and c_{55}^m are the density and the shear elastic stiffness of the m constituent. The subscripts/superscripts p and c indicate that the physical quantities are for the polymer and the ceramic, respectively. The requirements of the wave function ψ and the shear stress T_5 to be continuous at the ceramic-polymer interface lead to the following relations among the coefficients, A_n , B_n , C_n , and D_n , in the n th cell:

^{a)}Electronic mail: wcao@sun01.mrl.psu.edu

$$\begin{pmatrix} A_n \\ B_n \end{pmatrix} = \frac{1}{2Z_p} \begin{pmatrix} (Z_p + Z_c)e^{i(k_p - k_c)(nd-a)} & (Z_p - Z_c)e^{i(k_p + k_c)(nd-a)} \\ (Z_p - Z_c)e^{-i(k_p + k_c)(nd-a)} & (Z_p + Z_c)e^{i(k_p + k_c)(nd-a)} \end{pmatrix} \begin{pmatrix} C_n \\ D_n \end{pmatrix} = [T_{nd-a}] \begin{pmatrix} C_n \\ D_n \end{pmatrix}. \quad (4a)$$

Similarly, we can derive the relations among the coefficients C_n , D_n and A_{n+1} , B_{n+1} between adjacent cells,

$$\begin{pmatrix} C_n \\ D_n \end{pmatrix} = \frac{1}{2Z_c} \begin{pmatrix} (Z_p + Z_c)e^{i(k_c - k_p)nd} & (Z_c - Z_p)e^{i(k_c + k_p)nd} \\ (Z_c - Z_p)e^{-i(k_c + k_p)nd} & (Z_p + Z_c)e^{i(k_c + k_p)nd} \end{pmatrix} \times \begin{pmatrix} A_{n+1} \\ B_{n+1} \end{pmatrix} = [T_{nd}] \begin{pmatrix} A_{n+1} \\ B_{n+1} \end{pmatrix}, \quad (4b)$$

where

$$Z_m = \rho_m v_m = \sqrt{\rho_m c_{55}^m} \quad (m=p, c) \quad (5)$$

is the acoustic impedance and v_m is the acoustic velocity for material m . From Eqs. (4a) and (4b) we can derive the recurrence relation for the coefficients A_n and B_n ,

$$\begin{pmatrix} A_n \\ B_n \end{pmatrix} = [T_{nd-a}][T_{nd}] \begin{pmatrix} A_{n+1} \\ B_{n+1} \end{pmatrix}. \quad (6)$$

Considering a system of N cells, we can derive the following relation, according to the above recurrence relation:

$$\begin{pmatrix} A_1 \\ B_1 \end{pmatrix} = [T] \begin{pmatrix} A_{N+1} \\ B_{N+1} \end{pmatrix}, \quad (7)$$

where the T matrix in Eq. (7) is a second rank tensor given by

$$[T] = [T_{d-a}][T_d] \dots [T_{nd-a}][T_{nd}] \dots [T_{Nd-a}][T_{Nd}]. \quad (8)$$

For convenience, we assume that the composite is made of N cells and is immersed in a polymer medium. Since the incident wave enters the composite from the left, $B_{N+1} = 0$, in other words, only a transmitted wave exists in the medium on the right side of the composite.

Now, let us define a transmission function $H(\omega)$,

$$H(\omega) = \frac{A_{N+1} e^{-ik_p Nd}}{A_1} = \frac{1}{T_{11}} e^{-ik_p Nd}, \quad (9)$$

which describes both the amplitude and phase relationships between the incident wave at $x=0$ and the transmitted wave at $x=Nd$. Similarly, we can define a reflection function $G(\omega)$,

$$G(\omega) = \frac{B_1}{A_1} = \frac{T_{21}}{T_{11}}, \quad (10)$$

which describes the amplitude and phase relationships between the incident wave and the reflected wave at $x=0$.

Clearly, the transmission and reflection coefficients are (see the Appendix)

$$t = H(\omega) \cdot H^*(\omega) \quad (11)$$

and

$$r = G(\omega) \cdot G^*(\omega). \quad (12)$$

It is easy to verify that (see the Appendix)

$$t + r = 1. \quad (13)$$

In order to calculate the dispersion relation without using Floquet theory, an effective real wave vector k' needs to be defined for the composite, which should give the same phase change as $H(\omega)$ over a distance Nd . In this spirit, we introduce the following definition:

$$k' = \frac{\text{Ang}[H(\omega)]}{Nd} = \text{arctg} \left(\frac{\text{Im}[H(\omega)]}{\text{Re}[H(\omega)]} \right), \quad (14)$$

where $\text{Ang}[H(\omega)]$ represents the phase angle of $H(\omega)$.

Before we extract the stopband information from this new definition, let us examine the characteristics of the dispersion relation shown in Fig. 2, which is derived from the Floquet condition for an infinite system. The piecewise dispersion curve represents the passbands while the gaps are the stopbands. In each of the passbands, the phase velocity $v_{\text{ph}} = \omega/k$ is a monotonically decreasing function of frequency. v_{ph} is always a minimum at the upper passband edge frequency ω_p^U , and a maximum at the lower passband edge frequency ω_n^L .

The derivation of the band structures was based on the nonexistence of real k , and the band edges are those frequencies corresponding to the discontinuities of the dispersion relation.²² For a finite system, these discontinuities are expected to be smoothed out and solutions for the finite system should approach the discontinuity limit as the number of cells in the system becomes very large. We found that this goal can be precisely achieved using the new definition Eq. (14). One important point is that the newly defined k' will always have a finite value, although it may become extremely small in certain frequency regions when the system becomes very large. We will see later that the dispersion relation obtained from Eq. (14) approaches the Lee and Yang solution (Ref. 22) for very large systems.

Next, we need to define the bands using the new definition. In reference to the characteristics of the phase velocity in the band structure of Fig. 2, one may define the band structures of a finite system by using the maxima and the minima of the phase velocity $v_{\text{ph}} = \omega/k'$. These extrema can be easily calculated, and serve as the boundary mark between different frequency bands. For a finite system, the band structures will not be fully developed, they are pseudopassbands and pseudostopbands which have many similar characteristics as the true bands. A pronounced difference from the solution of Lee and Yang is that the phase velocity also can be defined inside the pseudostopbands.

Lee and Yang²² have shown that the wave number is purely imaginary inside a stopband for an infinite system. For a finite system, the real part of the wave number always exists even inside the pseudostopbands; therefore the wave number will be a complex number in general, i.e., $k = k' - ik''$. The imaginary part k'' may be calculated according to the following equation:

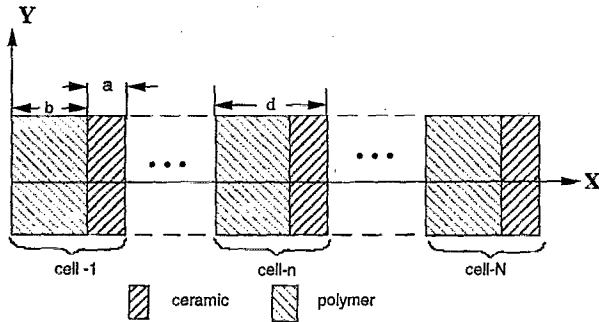


FIG. 1. Schematic plot of a N -cell 2-2 ceramic-polymer composite with $1/3$ of ceramic volume content. The y dimension is assumed to be infinite so that the system can be treated as one dimensional.

$$k'' = - \frac{\ln|H(\omega)|}{Nd}, \quad (15)$$

which can be nonzero inside the passbands for a finite system.

III. WAVE PROPAGATION IN A FINITE PERIODIC SYSTEM WITHOUT DAMPING

Using Eqs. (3), (4), (8), and (9), the transmission function $H(\omega)$ is calculated as a function of N for a system shown in Fig. 1. The volume content of the ceramic is fixed at $1/3$, i.e., $a/d=1/3$, and the material parameters used in the calculations are given in Table I.

Figures 3(a)–3(e) show the change of the magnitude of $H(\omega)$ as a function of frequency for composites of $N=1, 2, 10, 50$, and 100 . The frequency is normalized with respect to ω_0 , where ω_0 is defined as

$$\omega_0 = \frac{\pi v_c v_p}{b v_c + a v_p}, \quad (16)$$

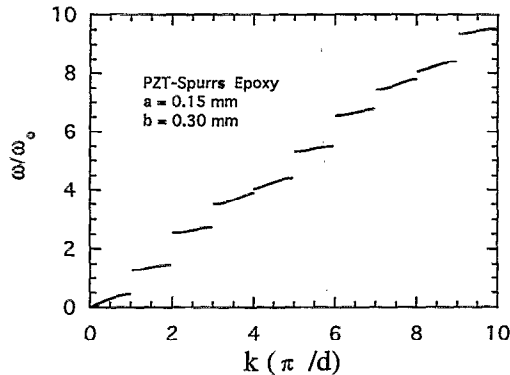


FIG. 2. Dispersion relation for an infinite system obtained from Floquet theory. The frequency unit $\omega_0 = \pi v_c v_p / (b v_c + a v_p) = 9491601/s$, v_c and v_p are the acoustic velocities of the ceramic and the polymer, respectively. The width of each stopband is different, which depends on both the degree of acoustic impedance mismatch and the volume content of ceramic.

TABLE I. Material properties for the ceramic and polymer constituents of the 2-2 composite.

Ceramic	$c_{55}^c = 2.4 (10^{10} \text{ N/m}^2)$, $\rho_c = 7800$
Polymer	$c_{55}^p = 1.59 (10^9 \text{ N/m}^2)$, $\rho_p = 1160$

v_c and v_p are the shear acoustic velocities of the ceramic and the polymer, respectively. The development of the band structures with the increase of cell number N can be seen clearly from Figs. 3(a) to 3(e).

It is interesting to note that some band structure characteristics start to show even for a single layer ceramic inclusion. Complete transmission, i.e., $|H(\omega)|=1$, can be achieved at isolated frequencies due to structural resonance. As the number of cells N increases, complete transmission occurs at more and more frequencies. Eventually, as N goes to infinity, true passbands are formed. The stopbands correspond to total reflection, i.e., $|H(\omega)|=0$. For a finite system such condition cannot be achieved; however, the value of $|H(\omega)|$ can become negligible inside the pseudostopbands.

When $N=10$, pseudostopbands are clearly visible but the passbands are not well defined. In general, it appears that the number of frequencies which allow the wave to pass

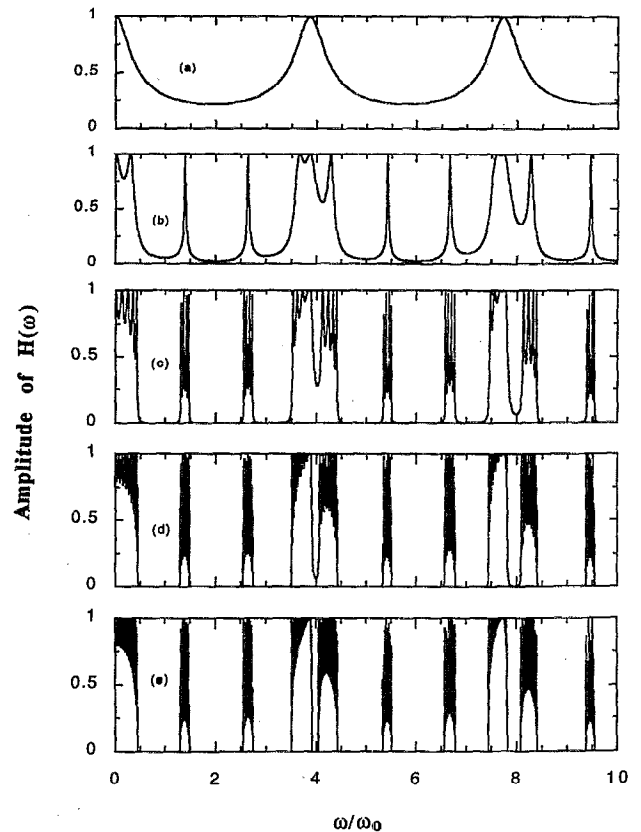


FIG. 3. The magnitude of transmission function vs frequency for different size composites. The development of band structure with the increase of number of cells N is calculated for the following cases: (a) 1 cell, (b) 2 cells, (c) 5 cells, (d) 10 cells, and (e) 50 cells.

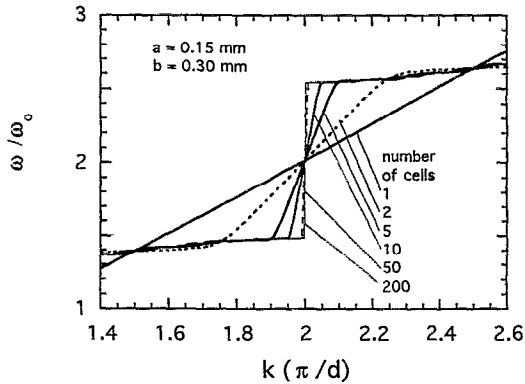


FIG. 4. The development of the second stopband with the increase of N . The deviation is quite large for systems containing less than 10 cells, but when N is greater than 200, the Floquet treatment can give reasonable description.

through the structure without reflection is equal to $N-1$. Therefore, it is conceivable that complete passbands will form only when $N \rightarrow \infty$.

This fact is seen more clearly in the dispersion relations depicted in Fig. 4. Using Floquet's condition, Lee and Yang²² have derived the dispersion relation for an infinite periodic system (see Fig. 2), sharp discontinuities occur at $k = n\pi/d$. While for a finite system, some degree of round off occur at these discontinuities. The edges of the passbands become sharper as the number of cells N increases (Fig. 4). When $N=200$, the dispersion relation almost coincides with that of an infinite system derived by Lee and Yang²² (see Fig. 4).

For an infinite system, one can derive the evanescent wave solutions for frequencies inside the stopbands using Floquet theory. The magnitude of these evanescent waves decays exponentially in space, but the phase angle, which is determined by the real part of the wave number, is independent of frequency ($k' = 0$). For a finite system, on the other hand, the real part of the wave number is always nonzero, hence, the phase angle will be frequency dependent inside the pseudostopbands. The decay of the magnitude is slower inside a pseudostopband than inside a true stopband. It is apparent that the band edges are not well defined when N is small, and gradually become sharper as N increases.

Figure 5 shows the vibration pattern at a given frequency inside a passband for composites with different numbers of cells. We can see the resonance nature of the patterns, with the polymer vibrating at much larger amplitude than the ceramic.

Figure 6 shows the comparison of the vibration patterns occurred in a ten-cell composite at three distinct frequencies. These three frequencies are selected as follows: $1.36364 f_0$ is in the first passband with a maximum value of $|H(\omega)|$, $1.55 f_0$ is at the upper edge of the first passband, and $2.009 f_0$ is at the center of the second stopband with a minimum value of $|H(\omega)|$. Different from the infinite system, there is no sharp edge between the passband and the stopband. As a result, a gradual transition can be seen from the passing resonant wave pattern to the localized evanescent wave pattern. The evanescent wave is practically localized within 2-3

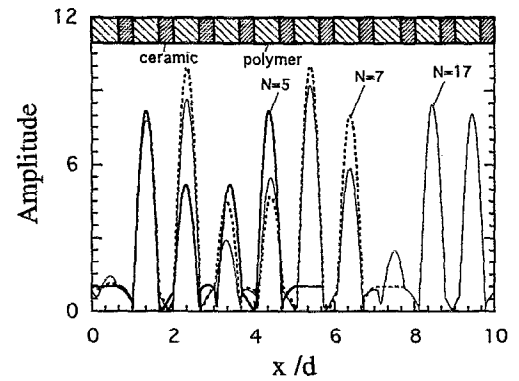


FIG. 5. Typical spatial vibration pattern for a completely transmitted wave with frequency in the first passband. The pattern changes for different N , the internal vibrational magnitude can be much larger than that of the incident wave and is also much larger in the polymer phase than in the ceramic phase.

cells. According to symmetry analysis on the vibration patterns shown in Fig. 7, the upper edge of the second stopband resonance is piezoelectrically active for the 1/3 ceramic volume percent composite, i.e., all the ceramic elements are vibrating in phase. Therefore, this mode will couple strongly to the thickness mode affecting the performance of a composite transducer.²⁶

It is a common practice to reduce the size of the composite cells in designing high-frequency composite transducers. The rule of thumb is that the upper edge of the second stopband resonance should be twice as high as the transducer operating frequency. This will place the thickness mode inside the first stopband of the transverse wave to minimize the coupling.⁴ In reality, there are technical limitations for making fine scale ceramic inclusions. An alternative to reduce the shear wave resonance effects is to introduce randomness into the composite structures, since randomness can destroy many shear resonance modes.²⁶⁻²⁹

IV. WAVE PROPAGATION IN APERIODIC FINITE SYSTEM

Theoretically speaking, true randomness can only be achieved in an infinite system. In reality, we seek wave localization which can be achieved with limited number of cells. The questions of interest are

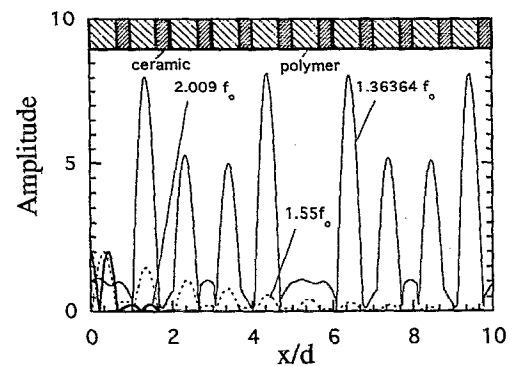


FIG. 6. Vibration pattern of a 10 cell composite. (—) A frequency in the passband. (—) A frequency in the pseudostopband. (---) A frequency near the edge of the pseudostopband.

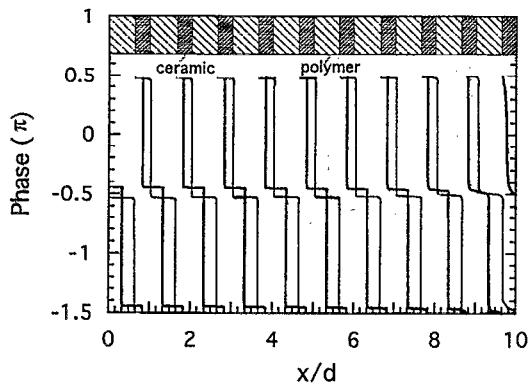


FIG. 7. Phase profiles for the upper and lower band edge frequencies of the second pseudostopband. (—) upper band edge frequency; (---) lower band edge frequency. The lower band edge frequency vibration is piezoelectric active since all the ceramics are in phase. Slight phase lagging occurred due to finite size, which can be seen by comparing the phase angle of the first layer and of the last layer.

- (1) How much randomness is sufficient?
- (2) What is the size dependence of the random effect?

With the 2-2 composite structure discussed above, these questions can be conveniently studied using the T -matrix technique plus the new definition of Eqs. (14) and (15). Both vibration profile and band structures can be calculated for an aperiodic 2-2 composite.

There are several ways to introduce randomness into a 2-2 composite. The simplest way is either randomizing the spacing between ceramic plates (randomizing b), or changing the ceramic plate thickness while leaving their spacing constant (randomizing a). Since the effects of randomization of b or a are similar due to the symmetry of the structure, we only give the results for randomizing b to illustrate the physical characteristics. When a or b is randomized, the number of passing frequencies will be greatly reduced and all the pseudostopbands become wider. The random effects are greatly enhanced when both a and b are randomized at the same time, with new characteristics produced as discussed below.

Figure 8 shows the comparison between the magnitudes of transmission function $H(\omega)$ for randomizing b , and for randomizing both a and b . The composite has 20 cells and the ceramic volume percent is kept at 1/3 on the average in order to compare with the results of the periodic composite calculated in Sec. III. An interesting fact in the case of randomizing b is that the transmission is not completely destroyed for all frequencies, there still exist some frequencies which allow the waves to completely pass through [$|H(\omega)| = 1$] as shown in Fig. 8. The reason is that a resonance length scale, i.e., the ceramic thickness a , still remains in the composite. Conversely, when randomness is introduced in both the ceramic thickness a and their spacing b , all but the first passband are eliminated. There appears to be a cut-off frequency for wave propagation in the random composite. Intuitively, the first passband should represent the propagation of waves with wavelengths comparable to and larger than the size of the composite system. The bandwidth is also expected to become narrower as the number of cells increases. How-

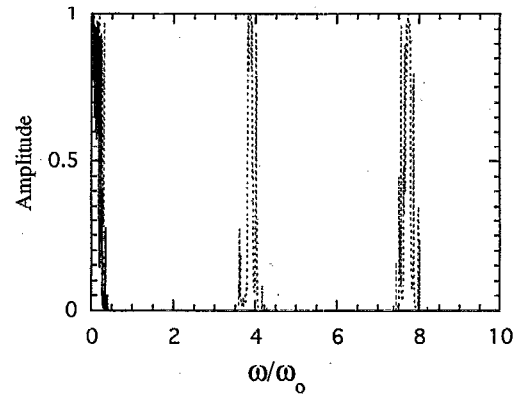


FIG. 8. The band structures for a randomly spaced ceramic plate composite (randomizing b , dashed curve) and a completely random composite (randomizing both a and b , solid curve), respectively. For the randomly spaced composite, the stopband width becomes much wider compared with the periodic structure, but there are still passing waves at higher frequencies. While for the completely random structure, no passing wave after a cut-off frequency.

ever, direct correlation between the dimension of the composite and the cut-off frequency was not found in our calculations.

An important point here is that the characteristics of localized waves in the random structure are quite different from those of the stopband waves. Although the magnitude of the waves shows exponential decay in space for both cases, the phase of the stopband waves is independent of frequency, while the phase of the localized waves shows strong frequency dependence. There are many stopbands in a periodic composite, each of the bands has a bandwidth characterized by the band edges. While in a random composite, the band structure consists of only one passband, no waves can go through the structure at frequencies above the cut-off frequency.

Considering the efficiency of cross-talking elimination, the stopband waves decay faster than the random localized waves, as illustrated in Fig. 9. The decay rate is the highest for the frequency at the center of each stopband; typically the wave vanishes in 2–3 cells. The decay rate becomes slower

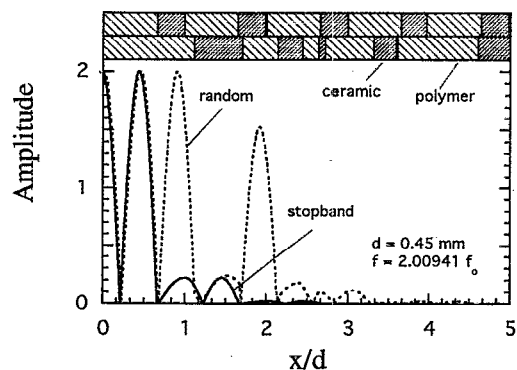


FIG. 9. Comparison of the transmission function for a periodic structure at a pseudostopband frequency and for a completely random structure at the same frequency.

as the frequency moves away from the center frequency of the stopband. On the other hand, localized waves are not so sensitive to frequency as long as the frequency is above the cut-off frequency. The localized waves have much broader bandwidth, although the decay rate for the localized waves is relatively slower than for the stopband waves. A typical localized wave can be confined within 6–7 cells. These quantitative evaluations can be used as general guidelines for the design of random composites.

V. SUMMARY AND CONCLUSIONS

We have studied shear wave propagation in a 2-2 composite structure using the T -matrix technique. A new definition is introduced for the effective wave number k [Eqs. (14) and (15)]. Using the new definition, the dispersion relation for a finite composite system is calculated without using the Floquet theory, which is valid only for an infinite system.

The formation of the band structures with the increase of composite cells can be seen clearly from the calculated results (Fig. 4). Our results show that the boundaries between stopbands and passbands become unclear for a finite system. Pseudostopbands can develop quickly with the increase in the number of cells in the composite. Stopband-like frequency regions are already formed in a composite of 10 cells as shown in Fig. 3. For a system with more than 200 cells, the dispersion relation calculated using the new definition is nearly identical with that obtained from Floquet theory (see Fig. 4).

Wave patterns inside the composites can be quite complicated and the magnitude of vibration could be much larger than the incident wave due to resonance. It is demonstrated that the polymers vibrate at much larger amplitude than the ceramics. These shear resonance modes are undesirable for thickness mode transducers because they not only reduce the efficiency of the transducer, but also prolong the ringdown in the pulse mode, producing poor resolution.

There are two ways to solve this problem: one is to reduce the cell dimensions, which can push the shear resonance to higher frequencies and place the operating frequency inside the first stopband to reduce the coupling;¹⁵ and the other is to introduce randomness into the structure, which can effectively destroy the shear resonance in a much broader band, and also can overcome the technical limitations encountered in fabricating fine scale composites. It is shown that the waves can be confined within 6–7 cells if both a and b are randomized. Therefore, this technique could be very useful and cost effective in producing high-frequency composite transducers of small size.

ACKNOWLEDGMENT

Financial support for this work is provided by the Office of Naval Research under Grant No. N00014-92-J-1501.

APPENDIX

From Eqs. (3) and (4) we have

$$|T_{nd-a}||T_{nd}| = 1, \quad (\text{A1})$$

so that

$$|T| = |T_{d-d}||T_d| \cdots |T_{nd-a}||T_{nd}| \cdots |T_{Nd-a}||T_{Nd}| = 1, \quad (\text{A2})$$

$$\begin{aligned} |T| &= T_{11}T_{22} - T_{12}T_{21} \\ &= T_{11}T_{11}^* \left(1 - \frac{T_{12}T_{12}^*}{T_{11}T_{11}^*} \right) = \frac{1}{t} (1-r) = 1, \end{aligned} \quad (\text{A3})$$

$$t+r=1.$$

Note $[T_n]$ is in the form of $\begin{bmatrix} T_{11} & T_{12} \\ T_{12}^* & T_{11}^* \end{bmatrix}$; therefore, the total matrix $[T]$ which is a product of each individual matrix also has the relation

$$T_{22} = T_{11}^*, \quad (\text{A4})$$

$$T_{21} = T_{12}^*, \quad (\text{A5})$$

$$\begin{aligned} \begin{pmatrix} a & b \\ b^* & a^* \end{pmatrix} \begin{pmatrix} c & d \\ d^* & c^* \end{pmatrix} &= \begin{pmatrix} ac+bd^* & ad+bc^* \\ b^*c+a^*d^* & b^*d+a^*c^* \end{pmatrix} \\ &= \begin{pmatrix} e & f \\ f^* & e^* \end{pmatrix}. \end{aligned} \quad (\text{A6})$$

- ¹A. Alippi, F. Cracium, and E. Molanari, *J. Appl. Phys.* **64**, 2238 (1988).
- ²A. Alippi, F. Cracium, and E. Molanari, 1988 IEEE Ultrasonics Symposium Proceedings, 1988, p. 623.
- ³A. Alippi, F. Cracium, and E. Molanari, *Appl. Phys. Lett.* **53**, 1806 (1988).
- ⁴W. A. Smith, A. A. Shaulov, and B. A. Auld, *Ferroelectrics* **91**, 155 (1989).
- ⁵W. A. Smith and B. Auld, *IEEE Trans. Ultrasonic, Ferroelectrics, and Frequency Control* **38**, 40 (1990).
- ⁶W. A. Smith, Proceedings of 1990 IEEE 7th International Symposium on Applications of Ferroelectrics (ISAF90) 1990, Vol. 145.
- ⁷G. Hayward and J. A. Hossack, *J. Acoust. Soc. Am.* **88**, 599 (1990).
- ⁸J. A. Hossack, B. A. Auld, and H. D. Batha, Proceedings of IEEE 1991 Ultrasonic Symposium, 1991, p. 651.
- ⁹C. G. Oakley, Ph.D. thesis, The Pennsylvania State University, 1991.
- ¹⁰Y. Wang, E. Schmidt, and B. A. Auld, Proceedings of IEEE 1986 Ultrasonic Symposium, 1986, p. 685.
- ¹¹K. Y. Hashimoto and M. Yamaguchi, Proceedings of IEEE 1986 Ultrasonic Symposium, 1986, p. 697.
- ¹²B. A. Auld, H. A. Kunkel, Y. A. Shui, and Y. Wang, Proceedings of IEEE 1983 Ultrasonic Symposium, 1983, p. 554.
- ¹³C. Potel and J. F. Belleval, *J. Acoust. Am.* **93**, 2669 (1993).
- ¹⁴Y. Wang and B. A. Auld, Proceedings of IEEE 1985 Ultrasonic Symposium, 1985, p. 637.
- ¹⁵B. A. Auld, Y. A. Shui, and Y. Wang, *J. Phys. (Paris)* **45**, 159 (1984).
- ¹⁶Y. Wang, Ph.D. thesis, Stanford University, 1986.
- ¹⁷J. A. Hossack and G. Hayward, *IEEE Trans. Ultrasonic, Ferroelectrics, and Frequency Control* **38**, 618 (1991).
- ¹⁸W. Friedrich, R. Lerch, K. Prestele, and R. Soldner, *IEEE Trans. Ultrasonic, Ferroelectrics, and Frequency Control* **37**, 248 (1990).
- ¹⁹H. L. W. Chan and J. Unsworth, *IEEE Trans. Ultrasonic, Ferroelectrics, and Frequency Control* **36**, 434 (1990).
- ²⁰C. G. Oakley, Ph.D. thesis, The Pennsylvania State University, 1991.
- ²¹W. T. Thomson, *J. Appl. Phys.* **21**, 89 (1949).
- ²²E. H. Lee and W. H. Yang, *SIAM J. Appl. Math.* **25**, 492 (1973).
- ²³V. K. Kinra and Eric L. Ker, *Int. J. Solid Struct.* **19**, 393 (1983).
- ²⁴A. M. B. Braga and G. Hermann, *J. Acoust. Soc. Am.* **91**, 1211 (1991).
- ²⁵R. Esquivel-Sirvent and G. H. Cocolezzi, *J. Acoust. Soc. Am.* **95**, 86 (1994).
- ²⁶B. A. Auld and J. A. Hossack, *Electron. Lett.* **27**, 1284 (1991).
- ²⁷P. Sheng and Z. Zhang, *Phys. Rev. Lett.* **57**, 1879 (1986).
- ²⁸T. R. Kirkpatrick, *Phys. Rev. B* **31**, 5746 (1985).
- ²⁹R. Esquivel-Sirvent and G. H. Cocolezzi, *J. Acoust. Soc. Am.* **95**, 86 (1994).